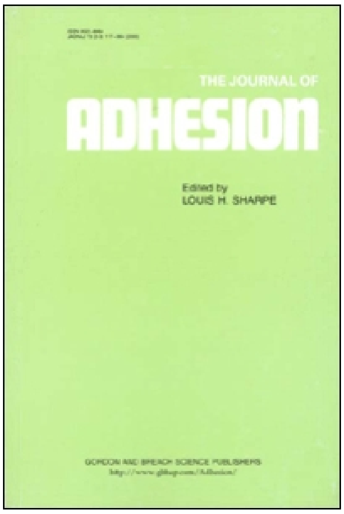

The Journal of Adhesion
Publication details, including instructions for authors and subscription information:
http://www.informaworld.com/smpp/title~content=t713453635

The Effects of Cure Temperature and Time on the Bulk Fracture Properties of a Structural Adhesive

Hooshang Jozavi[a]; Erol Sancaktar[a]
[a] Department of Mechanical and Industrial, Engineering Clarkson University, Potsdam, NY, U.S.A.

To cite this Article Jozavi, Hooshang and Sancaktar, Erol(1985) 'The Effects of Cure Temperature and Time on the Bulk Fracture Properties of a Structural Adhesive', The Journal of Adhesion, 18: 1, 25 — 48
To link to this Article: DOI: 10.1080/00218468508074935
URL: http://dx.doi.org/10.1080/00218468508074935

J. Adhesion, 1985, Vol. 18, pp. 25–48
0021-8464/85/1801-0025 $18.50/0

The Effects of Cure Temperature and Time on the Bulk Fracture Properties of a Structural Adhesive†

HOOSHANG JOZAVI and EROL SANCAKTAR

Department of Mechanical and Industrial Engineering Clarkson University Potsdam, NY 13676, U.S.A.

(*Received March 22, 1984; in final form July 11, 1984*)

The purpose of this investigation is to determine experimentally the possibility of optimizing the room temperature bulk fracture properties of structural adhesives with respect to cure temperature, time and cool-down conditions. The model adhesive, Metlbond, is a solid film modified nitrile epoxy resin supplied in two forms: Metlbond 1113 (supported with synthetic fabric carrier cloth) and Metlbond 1113-2 (without carrier cloth). The effects of carrier cloth on the bulk fracture properties are investigated as well. The uniaxial tensile strength and rigidity values were determined over a wide range of cure temperatures and times with fast and slow cool-down conditions during a previous investigation by the authors. For the present investigation, the fracture toughness of the model adhesives, subjected to opening mode failure, are experimentally determined, with the use of single-edge-cracked specimens, for different cure and cool-down conditions. It is found that the optimum fracture toughness values are obtained at low temperature-long time cure conditions in the absence of carrier cloth when slow cool-down condition is employed. Using the elastic-plastic material behavior assumption, it is shown that an average crack tip plastic zone radius can be determined using the fracture toughness and tensile strength values obtained corresponding to a given cool-down condition. These average plastic zone radii values are used along with the available tensile rigidity values to evaluate the optimum fracture energies of the model adhesives for a number of cure schedules. It is found that the optimum fracture energy levels are obtained at high temperature-short time cure conditions, using slow cool-down in the absence of carrier cloth.

† Presented at the Seventh Annual Meeting of The Adhesion Society, Jacksonville, Florida, U.S.A., February 13–15, 1984.

INTRODUCTION

The tensile strength and rigidity of adhesives are known to depend on the cure temperature, time and cool-down conditions.[1,2] Adhesively bonded joint failures are often results of catastrophic crack propagations (brittle fracture) originating from inherent flaws (voids or trapped air bubbles) and impurities.[3,4] These flaws are usually formed in the bulk of adhesive material rather than at the interface if ideal bonding and surface preparation of adherends prevail.[5] Hence, a complete characterization of adhesives requires investigation of flaw-related bulk material properties as well as bulk tensile properties as functions of cure and other service parameters.

A previous paper by the authors studied the effects of cure time and temperature as well as cool-down rate on the adhesive bulk tensile properties: yield stress (σ_y) and elastic modulus (E).[1] For this purpose cure temperature curves were plotted for different cure time conditions. These curves were typically "bell-shaped" exhibiting increasing – decreasing behavior of the tensile strength with respect to the cure temperature and hence revealing the existence of the maxima in such behavior. Envelope curves called the "optimization curves" were fitted through the maxima of these curves. Any maximum on these envelope curves represented the optimum point with respect to cure temperature and time. Commercially available, solid film Metlbond 1113 (with carrier cloth) and 1113–2 (without carrier cloth) adhesives were used as model adhesives. Among the conclusions of this work were the following:

- The ultimate strength and rigidity are higher at the cure conditions of low temperature-long time in comparison to the high temperature-short time on the optimization curves for Metlbond 1113 and 1113–2.
- For the adhesive with the carrier cloth (1113) the slow cool-down condition results in a higher ultimate strength and rigidity optimization behavior in comparison to the fast cool-down condition.
- For the adhesive without the carrier cloth (1113–2) the slow cool-down condition results in a higher ultimate strength behavior in comparison to the fast cool-down condition.
- The presence of carrier cloth results in higher tensile strength values when the fast cool-down condition is applied.

As mentioned previously, inherent flaws usually cause the bondline to fail in a brittle manner. Therefore, the use of an LEFM (Linear

Elastic Fracture Mechanics) approach can be considered appropriate for characterizing the fracture behavior of most adhesive materials. The dominant mode of failure for adhesive joints (particularly the single lap geometry) has been observed to be the opening mode (Mode-I).[6] Also, a recent investigation[7] on the cyclic debonding of adhesively bonded composites revealed that a debond always initiates and grows in the region of the highest G_I.

Based on the findings and considerations cited so far, investigation of K_{Ic} and G_{Ic} values for a model bulk adhesive became desirable. The model adhesives chosen for this project were Metlbond 1113 and 1113-2 which are commercially available from Narmco Materials, Inc. (Costa Mesa, California) in 0.01 in. (0.254 mm) and 0.005 in (0.127 mm) (respectively) thick solid film rolls. Metlbond 1113 is a 100% solids, modified nitrile epoxy film with a synthetic carrier cloth. Metlbond 1113-2 is identical to 1113 matrix without the carrier cloth. Metlbond 1113 was specifically developed to meet the stringent performance requirements of enhanced, bonded helicopter rotor blade structures. Both types of adhesives were chosen in order to obtain information on the effects of the carrier cloth at different cure conditions.

Metlbond 1113 and 1113-2 were used as model adhesives in a number of previous investigations.[1-4,8-11] These projects included tensile[1,2,10,11] and bonded fracture testing[8] of the same adhesive.

Brinson *et al.*[10,11] determined that the mechanical behaviour of bulk Metlbond 1113 and 1113-2 adhesives is affected by the rate of straining. They showed that the constant strain rate stress-strain behavior of the adhesives approaches an elastic-perfectly plastic behavior as the magnitude of the strain rate is increased. This mechanical behavior was described with the use of modified Bingham viscoelastic-plastic model.

The elastic-plastic material behavior assumption has been widely used by a number of investigators such as Bascom[6] and Hart-Smith[12] in the fracture studies of structural adhesives. Bascom used a crack tip plane-strain assumption to relate the adhesive tensile yield stress (σ_y), elastic modulus (E) and the crack tip plastic zone radius (r_{yc}) to the fracture energy (G_{Ic}). He calculated the plastic zone radius by using experimentally measured values of G_{Ic}, σ_y and E.[13-16] For a CTBN epoxy resin (Carboxy-Terminated Butadiene-Acrylonitrile), the magnitude of r_{yc} was calculated to be 7×10^{-3} in. (0.178 mm).[6,17] Bascom's results revealed that one can calculate G_{Ic} values directly from the tensile properties if information on the crack tip plastic zone radius is available.[1,2]

During the past few years, there have been a number of investigations on the variations of adhesive fracture energy with cure conditions. Koutsky *et al.*[18] examined the effects of cure time on the fracture energy (G_{Ic}) of a structural adhesive in the bonded form. They determined that as the cure time increases, the fracture energy reaches a maximum and then decreases. Higher cure temperatures appeared to accelerate this process.

The effects of cure cool-down conditions on the fracture energy (G_{Ic}) of Metlbond 1113-2 in the bonded form, have been investigated by O'Connor.[8] He determined that longer cool-down periods result in higher G_{Ic} values.

As mentioned earlier the present investigation is concerned with the study of model adhesives in the bulk form. However, in order to be able to interpret the bulk data to design bonded joints, one needs to understand the constraint mechanisms imposed on the adhesive material in the bonded form. Bascom[13] reports that the maximum fracture energy (G_{Ic}) for an adhesive in the bonded form was obtained when the bond thickness was approximately equal to the plastic zone diameter (2 r_{yc}). His investigations also revealed that this maximum G_{Ic} value was equal to that obtained with the bulk form of the adhesive.

The authors direct the reader to the reference by Kinloch[19] for further information on fracture behavior of adhesives.

OBJECTIVES

The objectives of this investigation were to:

1) Determine, experimentally, the fracture toughness (K_{Ic}) values for the model adhesives for different cure temperature, time and cool-down conditions.

2) Determine the dependence of crack tip plastic zone radius (r_{yc}) on the cure schedule and cool-down conditions.

3) Evaluate fracture energy values (G_{Ic}) based on the small-scale yielding elastic-plastic assumption using the measured tensile properties and average plastic zone radii values obtained with different cure and cool-down conditions.

4) Optimize the fracture toughness (K_{Ic}) and fracture energy (G_{Ic}) *vs.* cure temperature and time behaviors.

5) Determine the effect(s) of cool-down conditions on the fracture toughness and fracture energy-cure optimization behaviors;

6) Determine the effect(s) of the carrier cloth on the above mentioned optimization behaviors.

THEORETICAL CONSIDERATIONS

Irwin[20] showed that for an isotropic material in the bulk form the fracture toughness (K_{Ic}) can be related to the fracture energy (G_{Ic}) by

$$K_{Ic} = (G_{Ic}E')^{\frac{1}{2}} \tag{1}$$

where

$$E' = \frac{E}{1 - \nu^2} \tag{2}$$

for the plane strain condition and ν is the Poisson's ratio. He used the elastic-plastic material behavior assumption[21,22] and calculated the size (diameter) of the plastic deformation zone by considering an infinite plate containing a single crack under the action of tensile inplane loading perpendicular to the crack plane. The diameter of the plastic zone ($r_p = 2r_{yc}$) was shown to be

$$2r_{yc} = \frac{K_{Ic}^2}{\pi\sigma_y^2} \tag{3}$$

where σ_y is the uniaxial yield stress. Irwin also showed that the plane-strain elastic constraint increases the tensile yield stress for plastic yielding and thus affects the plastic zone size. Such an increase in the yield strength was estimated to be by a factor of $\sim(3)^{\frac{1}{2}}$.[22] Using this factor in Equation (3) results in

$$r_{yc} = \frac{1}{6\pi}\left(\frac{K_{Ic}}{\sigma_y}\right)^2. \tag{4}$$

Substitution of Equation (4) into Equation (1) yields

$$G_{Ic} = 6\pi\frac{\sigma_y^2}{E}r_{yc}\,(1 - \nu^2) \tag{5}$$

for the plane-strain condition. Equation (5) is especially useful for the present investigation as it relates bulk fracture and tensile properties.

Examination of literature reveals that the fracture toughness (K_{Ic}) and fracture energy (G_{Ic}) values have often been used interchangeably based on Equation (1) and linear elastic material assumption. Such an assumption allows the stress criterion and the energy criterion to be fulfilled simultaneously. A close scrutiny into their meanings and derivation, however, reveals that these two criteria need not be satisfied simultaneously when the yield stress and elastic modulus are different functions of the material process conditions (such as the cure parameters) or environmental conditions (such as humidity, temperature, radiation etc.).

The crucial difference between the two criteria can be explained with the following arguments: i) The energy criterion may be a necessary but not sufficient condition for crack extension. Such a situation may arise when the material at the crack tip is not ready to fail due to high yield stress even though sufficient energy for crack propagation is provided. ii) The stress intensity factor criterion may be the necessary but not sufficient condition for crack extension. Such a situation may arise when sufficient energy for the failure of material at the crack tip is not provided due to high modulus of elasticity.

Apparently, both of these possibilities should be taken into consideration when the yield stress and modulus of elasticity are different functions of process or environmental conditions. Consequently, when K_{Ic} and G_{Ic} values are maximized and minimized at different (cure) conditions the design criterion should dictate avoiding the relative minimum rather than choosing the absolute maximum.

EXPERIMENTAL PROCEDURE

Examination of the literature[8,13,15,16,23] reveals that the simplest method for the experimental determination of G_{Ic} is the use of the TDCB (Tapered Double Cantilever Beam) specimen geometry which was originally proposed by Mostovoy *et al.*[24] In TDCB specimens the rate of change of compliance is a constant value which is independent of the crack length due to the pesence of a "height" taper. The thickness requirement for this geometry has been suggested to be 0.5 in (12.7 mm) and above for application to bulk adhesive materials.[24]

Initial attempts to manufacture bulk TDCB specimens from the model adhesives proved unsuccessful due to the following reasons: i) Extremely large number of voids were produced during the curing process because of the large size of the TDCB specimen. ii) Significant amount of adhesive material had to be consumed to produce specimens, again due to the large specimen size. Consequently, another specimen geometry, which would avoid these difficulties, had to be chosen.

Specimen Geometry

ASTM standards[25,26] provide a number of specimen geometries to determine the fracture toughness (K_{Ic}) of bulk materials. Among them, the single-edge-cracked specimen geometry appears to be the smallest and simplest geometry as far as the preparation and testing of the specimens are concerned. Because of these reasons, the single-edge-cracked specimen geometry shown in Figure 1 was chosen to evaluate the bulk fracture toughness of the model adhesives.

The pertinent dimensions of plate specimens for K_{Ic} testing are the

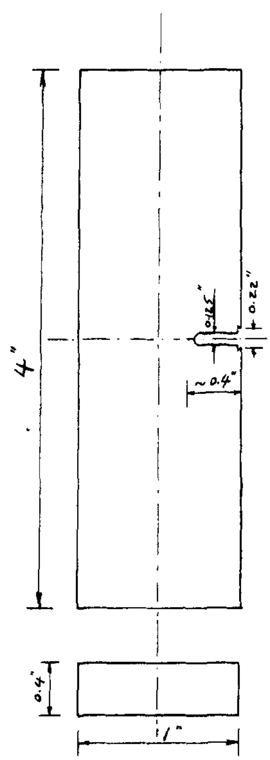

FIGURE 1 Single-Edge-Crack Specimen Geometry used for Fracture Toughness (K_{Ic}) Measurements.

crack length, thickness and the ligament (uncracked) length. According to References 25 and 26, for a K_{Ic} test to be valid, these dimensions should exceed a certain multiple of the quantity $\left(\frac{K_{Ic}}{\sigma_y}\right)^2$. This quantity has been shown[21] to be directly proportional to the crack tip plastic zone radius r_{yc} defined by equations (3) and (4). Based on the elastic-plastic material assumption, the LEFM solutions are valid beyond the plastically deformed zone around the crack tip, if the size of this zone is small.

Examination of the literature[25,26] reveals that the minimum values for specimen thickness and crack length are given by:

$$a, B \geqslant 2.5\left(\frac{K_{Ic}}{\sigma_y}\right)^2. \tag{6}$$

For the model adhesives of this investigation, a number of trial thicknesses were used in order to evaluate valid K_{Ic} values to satisfy Equation (6). A thickness of 0.4 in. (10.16 mm) was found to meet the standard requirements of valid K_{Ic} testing.[25,26] It was observed that smaller thicknesses resulted in much higher toughness values due to plane stress conditions. Thicker specimens, on the other hand, were found to have large number of voids produced during the cure process and considered undesirable.

Cure Schedules

Manufacturer's product information for the model adhesives[27] states that in the bonded form typical mechanical properties can be obtained with the following cure conditions:

	Low Temperature Cure	Standard Cure	Fast Cure
Temperature (°F)	200	260	290
(°C)	(93)	(127)	(143)
Time (Minutes)	120	30	20
Pressure (Psi) (vented)	15–50	15–50	15–50
(KPa)	(103–345)	(103–345)	(103–345)

For the present investigation a wider cure schedule range was chosen to understand better the adhesive behavior at extreme and intermediate conditions.

For this purpose the following cure time-temperature schedules were applied:

Cure Time (Minutes):	Cure Temperature (°F) (°C)					
120	200, (93)	230, (110)	260, (127)	290 (143)		
1000	170, (77)	200, (93)	230, (110)	260, (127)	290 (143)	
5000	140, (60)	170, (77)	200, (93)	230, (110)	260, (127)	290 (143)
10,000	115, (46)	140, (60)	200 (93)			

Cure time can be described as the amount of time the specimen is in the oven at a pre-set cure temperature level. Initially the oven is at room temperature (72°F–22°C) and the humidity level (RH) is at 65%. The specimen is heated at a rate of 10°F/min (5.5°C/min). For short cure times, the adhesive system temperature variations are approximately simulated by wrapping several layers of the adhesive around the oven thermocouple tip. For long cure times (*e.g.* 1000, 5000 and 10,000 minutes) the adhesive system temperature variation is monitored using several thermocouples at different locations and is observed to be the same as oven temperature during the major portion of the cure time. Cure time starts when the oven temperature reaches the cure temperature level. When the desired cure duration is completed, the oven is turned off and the specimen is allowed to cool-down either quickly (fast cool-down condition) or slowly (slow cool-down condition). The fast cool-down condition is simulated by taking the specimen out of the oven and letting it cool down to the room temperature. The variation of adhesive temperature in time was measured for the fast cool-down condition using an iron-constantan thermocouple, embedded in the middle of the adhesive layers, and it is shown in Figure 2. The slow cool-down condition is applied by leaving the specimen in the oven with its access door closed until the oven temperature reaches the ambient temperature. The variation of oven temperature in time for the slow cool-down condition is shown in Figure 3.

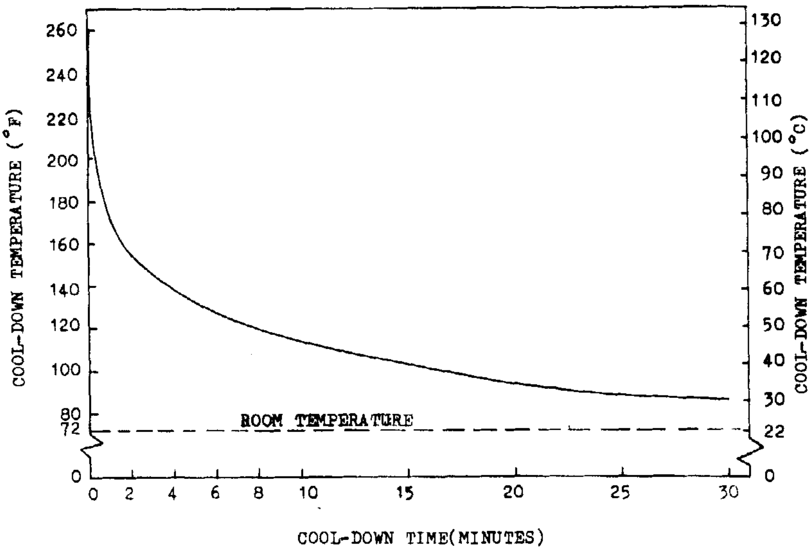

FIGURE 2 Temperature Decrease *vs.* Time for the Fast Cool-Down Condition.

Curing was performed using an ATS oven (Series 2911) equipped with a Dual Setpoint Temperature Controller (Series 2931).

Specimen Preparation

Metlbond 1113 and 1113-2 adhesive rolls were stored in a freezer at 30°F (−1°C) and ~0% RH. First, the adhesive roll was taken out of the freezer and allowed to thaw in the ambient temperature until it was flexible enough to work with. It was determined that for Metlbond 1113 (with carrier cloth) 45 layers and for Metlbond 1113-2 (without carrier cloth) 78 layers were needed to make thickness of 0.4 in. (10.16 mm) of cured material. Each layer was cut to 1.5 in. × 13 in. (38 mm × 330 mm) size. Two aluminum plates with 0.2 in. × 1.5 in. × 13 in. (5 mm × 38 mm × 330 mm) grooves were sprayed with Teflon and were used to cast the multilayered adhesive. For this purpose, the adhesive layers were carefully laid on one grooved plate and smoothened. The second plate was then placed on top of the first one and the two plates were tightly and uniformly clamped together. The assembly was subsequently placed in the oven for curing.

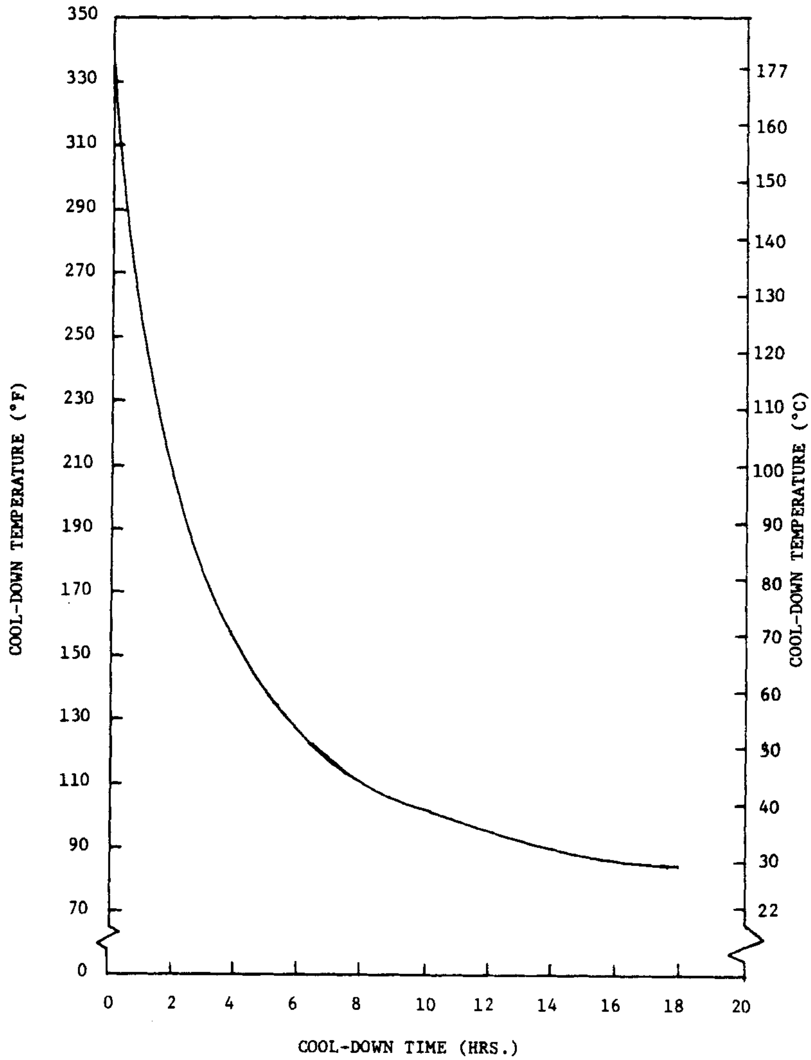

FIGURE 3 Temperature Decrease *vs.* Time for the Slow Cool-Down Condition.

At the end of the cure cycle, the assembly was cooled either quickly or slowly to simulate the fast and slow cool-down conditions.

For each cure condition three specimens were manufactured. In order to facilitate the machining of the specimens, the cured adhesive plate was taped to a metal specimen template using two-sided tape. A vertical contour saw was used to remove most of the excess adhesive along the template border. The final contour shaping was done by using a carbide-bit router as the template slided along a guide pin to ensure a uniform specimen shape. Finally the surfaces of the specimen were smoothened with a fine grade sanding block. The starter crack was produced subsequently by tapping a sharp knife at the base of the machined notch. The knife-edge at the mouth of the machined notch (Fig. 1) was made to facilitate mounting of a Crack Opening Displacement (C.O.D.) gage which was used in determining the K_{Ic} values. The final specimen dimensions are shown in Figure 1.

Several measurements had to be made before testing a specimen. The width and thickness were accurately measured using a micrometer. The total crack length (including the depth of machined notch and starter crack) was measured using a light reflective microscope at a magnification of 10X. This was done on both sides of the specimen and an average crack length value was calculated.

Testing and K_{Ic} Evaluation

All fracture toughness tests were performed using a Tinius-Olsen testing machine in an environment of ~72°F (22°C) and 65% RH. Each specimen was tested under uniform tension with a constant cross head rate of 2 in/min (50 mm/min). Such a fast head rate was used to minimize the viscoelastic effects. An Instron (series 2670) C.O.D. gage was placed on the specimen to monitor the crack opening displacement during the test. The output of the C.O.D. gage was amplified through a Vishay bridge amplifier and recorded on a strip chart recorder. The load *vs.* time data was recorded by a strip chart recorder supplied with the testing machine. Specimens were loaded up to complete fracture.

K_{Ic} evaluation is done using the procedure suggested by the ASTM standard[26] in the following manner. The load (P) *vs.* C.O.D. displacement (σ) curve is plotted first. A secant line is drawn through the origin of the test record with a slope 5% less than that of the linear portion of the record. The load level defined by the intersection point is assumed to correspond to initial crack growth and is used as the critical load in K_{Ic} evaluation.

For the model adhesives in this investigation, the P *vs.* σ records were observed to be linear up to fracture, as obtained with a number of cure conditions. In those cases the maximum load was chosen as the critical load.

The relation which correlates the stress-intensity factor with the specimen dimensions and applied load is called the K-calibration. For the single-edge crack geometry used for this project Gross *et al.*[28] applied a boundary collocation procedure to the Williams stress function[29] to determine the elastic stress distribution at the tip of an edge crack in a finite-width specimen subjected to uniform tensile loading. The K-calibration for the single-edge-crack geometry is given by

$$Y = \frac{K_{Ic}Bw}{P_c a^{\frac{1}{2}}} = 1.99 - 0.41\ (a/w) + 18.7\ (a/w)^2 - 38.48\ (a/w)^3 + 53.85\ (a/w)^4 \qquad (7)$$

where w is the specimen width and a is the crack length including the notch and the starter crack. Valid K_{Ic} values satisfied Equation (6) based on the σ_y values available as a result of our previous investigation;[1,2] the invalid K_{Ic} values were discarded.

RESULTS AND DISCUSSION

Figures 4 and 5 show the effects of cure time and temperature on the fracture toughness (K_{Ic}) of Metlbond 1113 and 1113-2, respectively, for the fast cool-down condition. Corresponding to each cure time, the K_{Ic} data are shown for a number of cure temperatures. Investigation of individual curves reveals the increasing-decreasing behavior of the fracture toughness with respect to cure temperature. This behavior is similar to the variation of yield strength with cure temperature for both adhesives.[1,2] The similarity of toughness-temperature and strength-temperature behaviors may be explained by considering Equation (4). Based on this equation, K_{Ic} is proportional to the yield strength (σ_y) and the square root of the plastic zone radius (r_{yc}). Therefore, the effect of variations in r_{yc} with cure temperature on the K_{Ic} is not as strong as that of yield strength. In other words, the variations of K_{Ic} and σ_y with cure temperature are similar. Figures 4 and 5 also show the toughness-cure optimization behaviors of the model adhesives. It can be observed that the optimum K_{Ic} values decrease for shorter cure times and higher cure temperatures. This behavior, also, is similar to the tensile strength-cure optimization behavior. Comparison of Figures 4

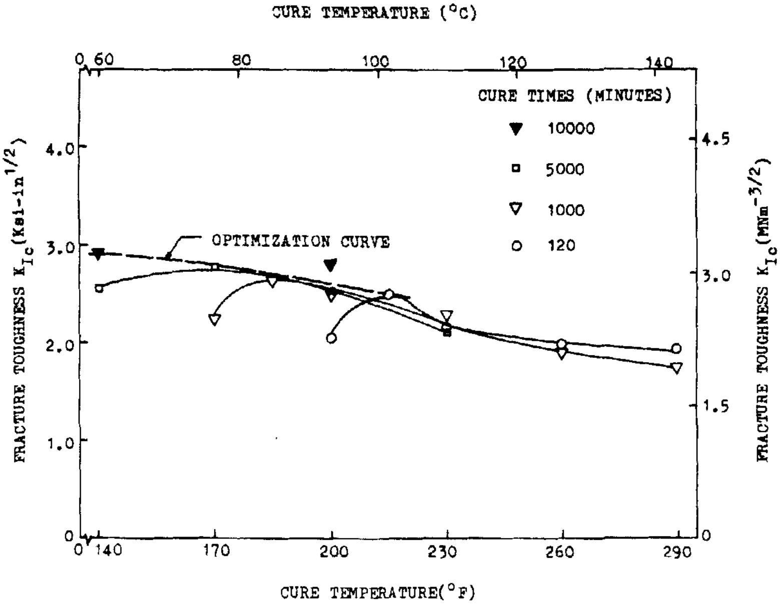

FIGURE 4 Metlbond 1113 Fracture Toughness-Cure Optimization Curve for the Fast Cool-Down Condition.

and 5 reveals the effect of carrier cloth on the fracture toughness-cure optimization behaviors of the adhesives. The K_{Ic} values of Metlbond 1113-2 (without carrier cloth) are affected less by the cure conditions in comparison to those for Metlbond 1113 particularly at low temperatures. This behavior may be attributed to the strengthening effect of carrier cloth by means of an increase in σ_y[10] and also to the fact that the presence of fibers causes the crack arrest mechanisms to prevail thus resulting in higher K_{Ic} values.

Figure 6 shows the effects of cool-down conditions on the Metlbond 1113 fracture toughness-cure optimization behavior. Apparently the slow cool-down condition yields higher K_{Ic} values. The difference in K_{Ic} values for the two cool-down conditions is higher at high cure temperature-low cure time conditions. This can be explained by the fact that the magnitude of residual stresses created in the bulk of the adhesive material is larger at higher temperature-shorter time cure conditions due to high temperature gradients. Figure 7 shows the effect of cool-down conditions on the toughness-cure optimization behavior of Metlbond 1113-2. Again, it can be seen that the slow cool-down

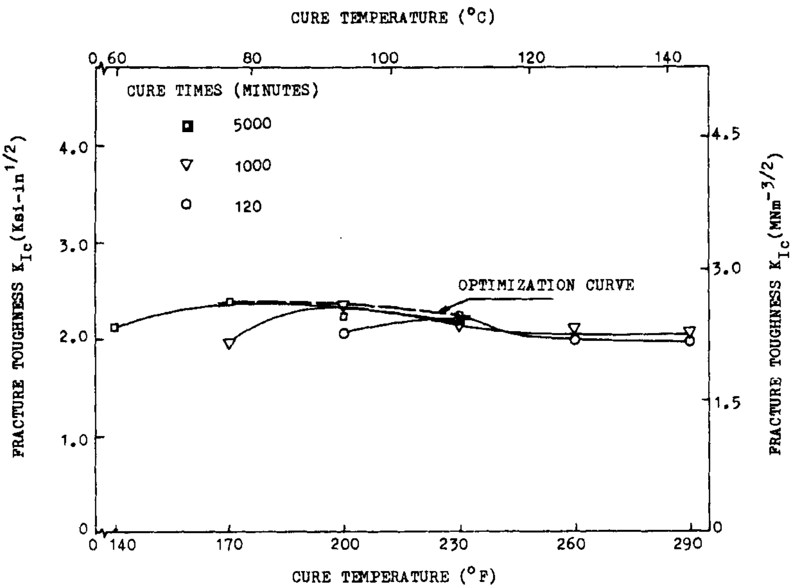

FIGURE 5 Metlbond 1113-2 Fracture Toughness-Cure Optimization Curve for the Fast Cool-Down Condition.

condition results in higher optimum K_{Ic} values as the rate of cooling decreases. Comparison of Figures 6 and 7 reveals some interesting facts regarding the effects of carrier cloth on optimum K_{Ic} values. Comparison of the fast cool-down optimum K_{Ic} values for Metlbond 1113 and 1113-2 adhesives reveals that the presence of carrier cloth results in higher fracture toughness values for Metlbond 1113; for the slow cool-down condition, however, relatively higher optimum K_{Ic} values are obtained in the absence of carrier cloth. This combined effect of carrier cloth and cool-down conditions is more significant at higher cure temperature-shorter cure time conditions. The above observations may be explained as follows: i) In the fast cool-down condition, the magnitude of the thermal residual stresses in Metlbond 1113-2 is higher than in Metlbond 1113 as a larger volume of adhesive material is used in the former. Furthermore, the carrier cloth serves as a stabilising agent and results in higher K_{Ic} values for Metlbond 1113; ii) By using the slow cool-down condition, however, the strengthening effect of carrier cloth (in Metlbond 1113) is superseded by the release of the residual stresses in Metlbond 1113-2 and results in a more uniform molecular structure

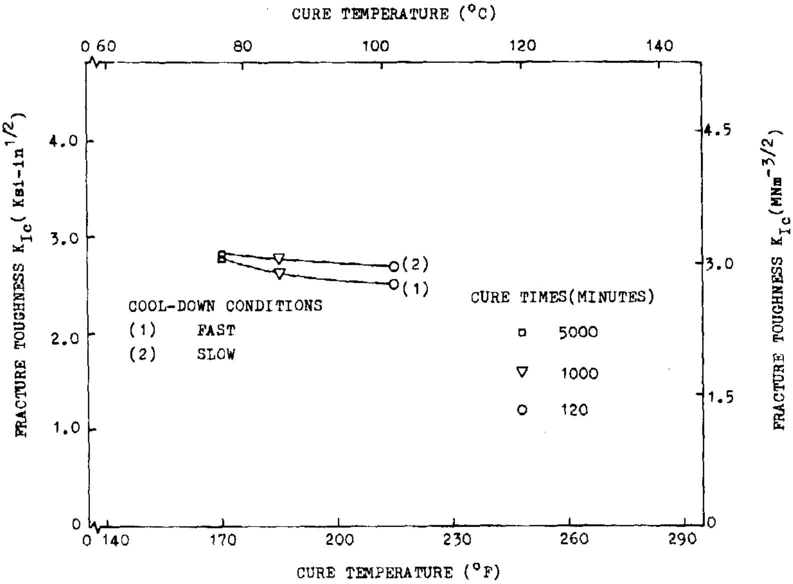

FIGURE 6 Comparison of Metlbond 1113 Fracture Toughness-Cure Optimization Curves for the Slow and Fast Cool-Down Conditions.

and therefore higher optimum K_{Ic} values for Metlbond 1113-2.

As mentioned earlier, information on the size of the crack tip plastic zone radius (r_{yc}) makes it possible to relate the bulk tensile properties to fracture properties in the form of fracture toughness (K_{Ic}) and fracture energy (G_{Ic}). Such a relation is possible on the basis of a "small scale" yielding assumption[19] and Equations (4) and (1). Figures 8 and 9 show the effects of cure conditions on the plastic zone radius (r_{yc}) of Metlbond 1113 and 1113-2, respectively. The r_{yc} values were obtained by using Equation (4) which incorporated the measured K_{Ic} (fracture toughness) and σ_y (tensile strength) data[1,2] for both adhesives. Figures 8 and 9 also show (dashed lines) the r_{yc} values corresponding to optimum K_{Ic}'s for the fast or slow cool-down conditions are relatively constant. Therefore it seems possible that one can use some average r_{yc} values (based on optimum K_{Ic}'s) to represent the typical plastic zone radii sizes for either material subjected to the fast or slow cool-down conditions. Using this concept, it can be seen in Figure 9 that the average plastic zone radius ($\bar{r}_{yc}$) for Metlbond 1113-2 with the slow cool-down condition is higher than that for the fast cool-down

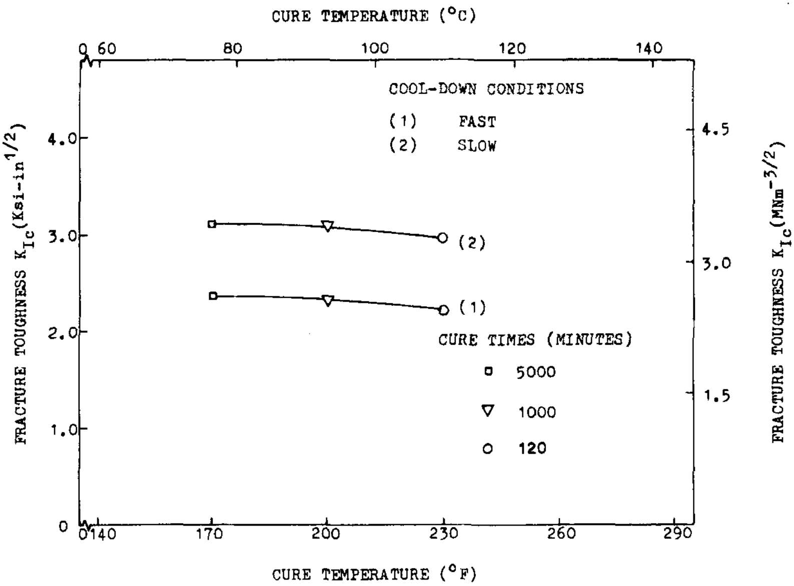

FIGURE 7 Comparison of Metlbond 1113-2 Fracture Toughness-Cure Optimization Curves for the Slow and Fast Cool-Down Conditions.

condition. As expected, this implies that the slow cool-down condition results in tougher adhesive matrix material (see Figure 7), as the availability of a larger plastic zone size at the crack tip enables relieving of higher stress levels at that location thus resulting in higher crack growth resistance. It is not possible to offer a similar argument for the adhesive with the carrier cloth as the $\bar{r}_{yc}$ values obtained with slow and fast cool-down conditions are about the same (Fig. 8). This result, however, is also expected since it is already known that the effect of cool-down conditions on Metlbond 1113 fracture toughness is minimal (Fig. 6).

Average plastic zone radii ($\bar{r}_{yc}$) values were calculated for Metlbond 1113 and 1113-2 adhesives by using the extreme r_{yc} values for the fast cool-down conditions. These calculations resulted in $\bar{r}_{yc}$ values of 6.88×10^{-3} in. (0.175 mm) for the 1113 and 5.83×10^{-3} in. (0.148 mm) for the 1113-2. For the slow cool-down condition, a simple averaging procedure for the more uniform r_{yc} values resulted in $\bar{r}_{yc}$ values of 6.76×10^{-3} in. (0.172 mm) for Metlbond 1113 and 8.63×10^{-3} in. (0.219 mm) for Metlbond 1113-2.

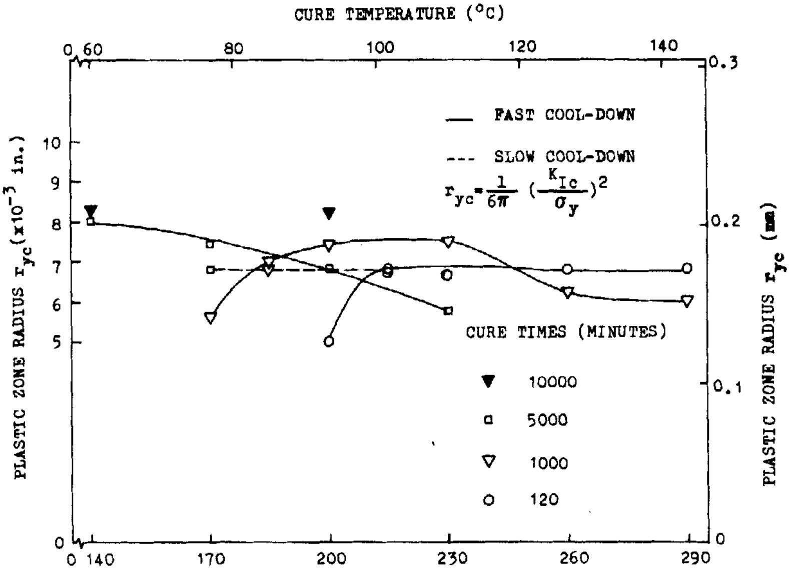

FIGURE 8 Effect of Cure Conditions on the Plastic Zone Radius Based on Bulk Tensile and Fracture Toughness Data of Metlbond 1113.

The availability of these $\bar{r}_{yc}$ values along with previously measured σ_y and E data[1,2] made the calculations of G_{Ic} values possible, based on Equation (5). These calculated values could also be compared with the G_{Ic} values which would be obtained on the basis of measured K_{Ic} values and Equation (1). In calculating fracture energies based on Equations (5) and (1), the value of Poisson's ratio (ν) was assumed to be the constant value of 0.374 for both materials.[10] Figures 10 and 11 show the effects of cure conditions on the fracture energy (G_{Ic}) of Metlbond 1113 and 1113-2, respectively, based on bulk tensile and fracture toughness data. In Figure 10, curves (1) and (2) represent the optimum G_{Ic} values for Metlbond 1113 based on equation (1). Curves (3) and (4) (Fig. 10) were plotted based on Equation (5) which incorporated the average plastic zone radii ($\bar{r}_{yc}$) and the bulk tensile properties. The same procedure was applied to Metlbond 1113-2 data to result in Figure 11. Comparison of Figures 10 and 11 confirms that: i) With the fast cool-down condition Metlbond 1113 yields higher G_{Ic} values than Metlbond 1113-2; ii) With the slow cool-down condition

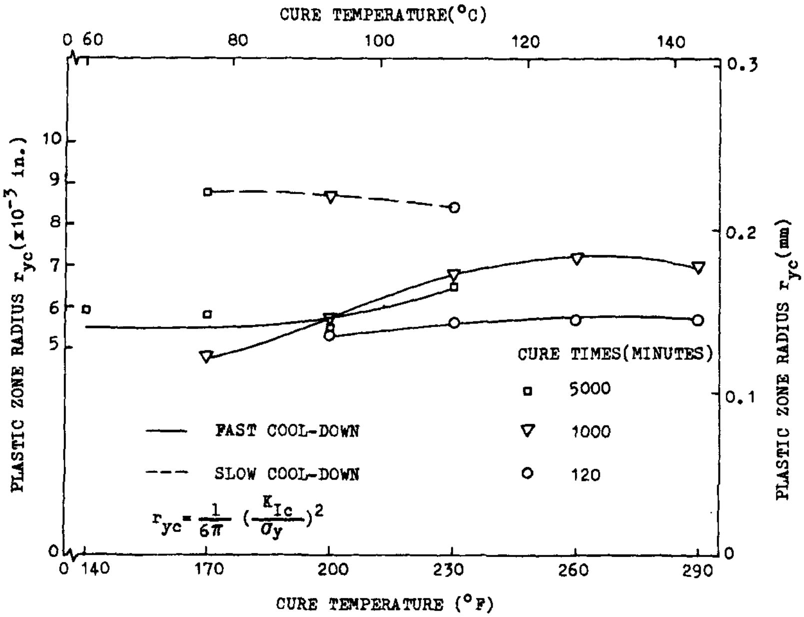

FIGURE 9 Effect of Cure Conditions on the Plastic Zone Radius Based on Bulk Tensile and Fracture Toughness Data of Metlbond 1113-2.

the optimum G_{Ic} values are significantly higher using Metlbond 1113-2 as compared with Metlbond 1113; iii) Cure temperature and time do not seem to have a significant effect on fracture energy for either material; iv) There is a better agreement between the optimum G_{Ic} values using Equations (1) and (5) for Metlbond 1113-2 than for Metlbond 1113.

CONCLUSIONS

The present investigation has been concerned with the experimental determination of the effects of cure temperature, time and cool-down conditions on the room temperature bulk fracture properties of the structural adhesives Metlbond 1113 (with carrier cloth) and 1113-2 (without carrier cloth). The effects of carrier cloth on the above-mentioned properties have been investigated as well.

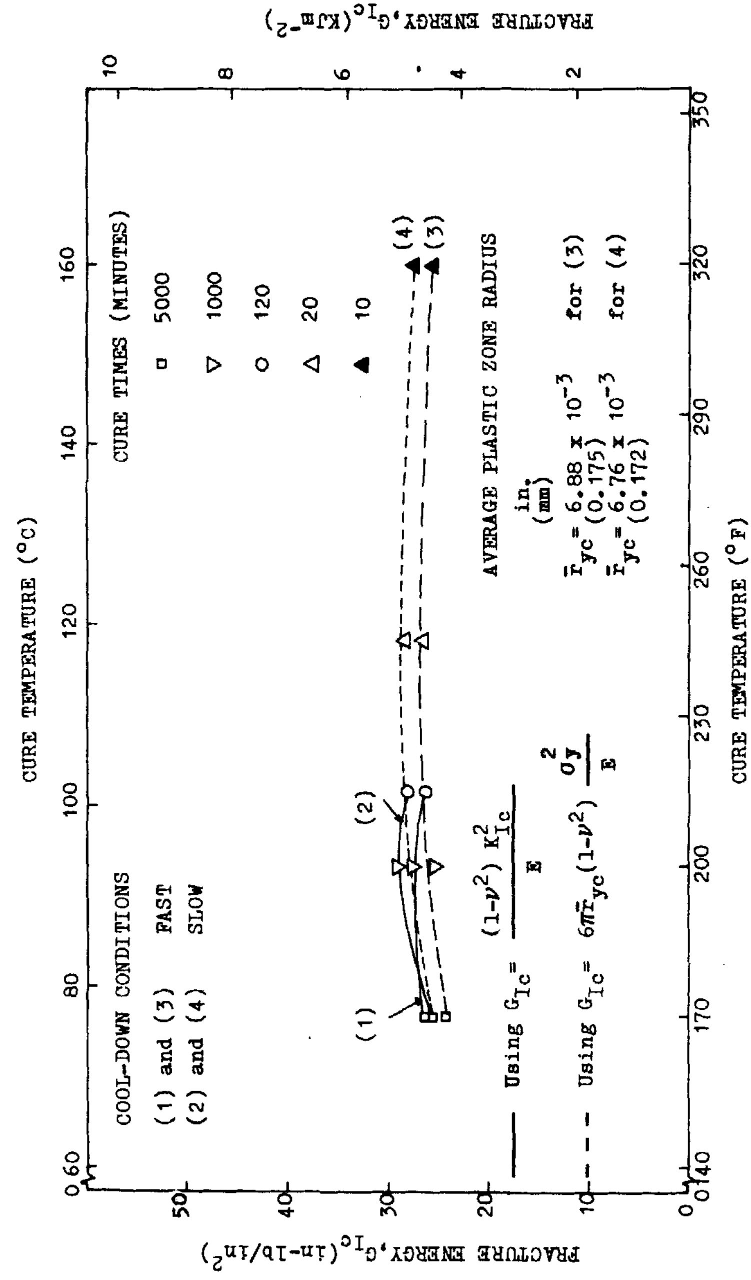

FIGURE 10 Metlbond 1113, Slow and Fast Cool-Down, Fracture Energy-Cure Optimization Curves Calculated Based on Bulk Tensile and Fracture Toughness Data.

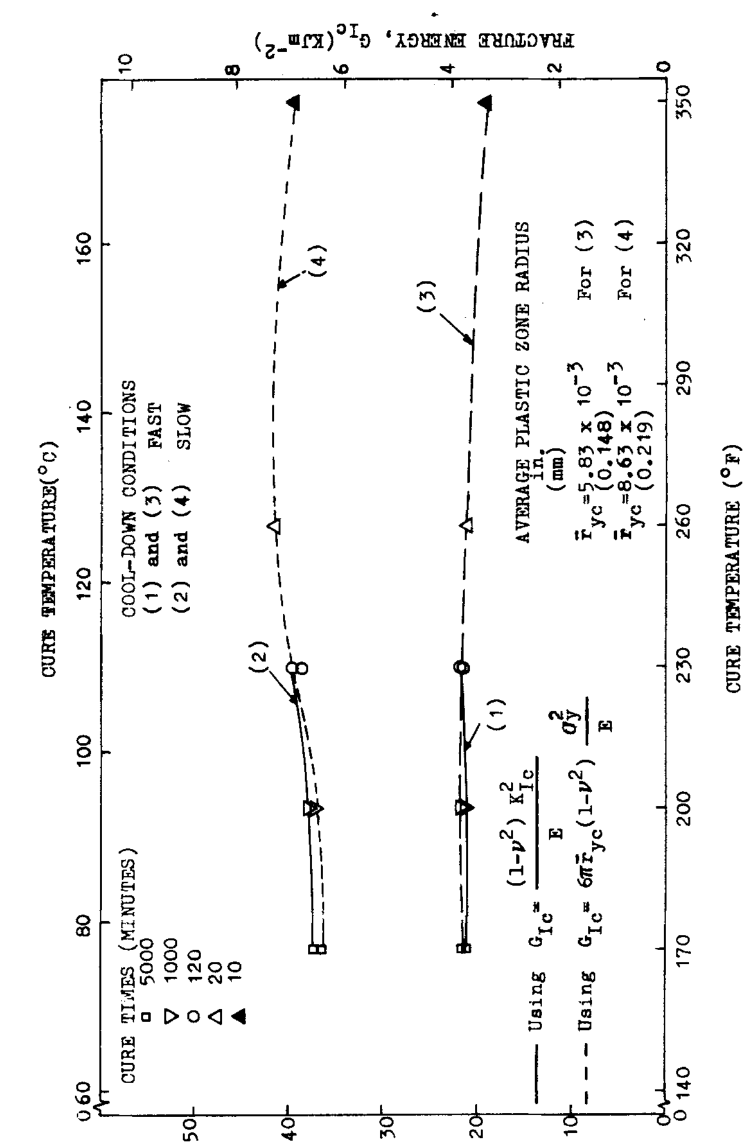

FIGURE 11 Metlbond 1113-2, Slow and Fast Cool-Down, Fracture Energy-Cure Optimization Curves Calculated Based on Bulk Tensile and Fracture Toughness Data.

In summary of the achievements of this study, the following conclusions can be made:

1) When the fast cool-down condition is employed, both adhesives yield higher optimum K_{Ic} values corresponding to lower temperature-longer time cure conditions. The variation of optimum K_{Ic}'s is less significant in the absence of the carrier cloth.

2) For both adhesives, slow cool-down condition yields higher optimum K_{Ic}'s as compared to those obtained with fast cool-down condition.

3) The effect of carrier cloth seems to result in higher optimum K_{Ic}'s with fast cool-down condition and lower values with slow cool-down condition.

4) Based on the elastic-plastic material behavior assumption and crack tip plane-strain condition (Equation 4) and for a fixed cool-down rate, an average plastic zone radius ($\bar{r}_{yc}$) may be calculated for either adhesive as a fracture property.

5) The use of slow cool-down condition increases the $\bar{r}_{yc}$ value by as much as 48% in the absence of carrier cloth. The presence of carrier cloth results in minimal change in $\bar{r}_{yc}$ with respect to cool-down conditions.

6) The bulk tensile properties such as strength and rigidity can be utilized to obtain a measure of the fracture energy (G_{Ic}) (using Equation 5) for different cure temperatures and times by assuming $\bar{r}_{yc}$ values to be material constants for given cool-down conditions (also see References 1 and 2). Consequently, the optimum G_{Ic} values may be calculated with the use of optimum bulk tensile properties.

7) The optimum G_{Ic} values are obtained with high temperature-short time cure conditions. The presence of carrier cloth seems to increase the optimum G_{Ic} values when the fast cool-down condition is used and decrease them when the slow cool-down condition is used.

8) The G_{Ic} values for Metlbond 1113-2 adhesive (without the carrier cloth) measured using bonded TDCB specimens[8] and single-edge-crack bulk specimens (the present investigation) show good agreement.

Further investigation may be to evaluate the fracture toughness (K_{Ic}) and fracture energy (G_{Ic}) values as functions of cure parameters for the model adhesives in the bonded form. It should also be noted that for Metlbond 1113 adhesive (with carrier cloth) in the bonded form, the plane of the crack propagation is likely to be parallel to that of the carrier cloth,[8] whereas in the bulk form it is perpendicular to the plane of the carrier cloth. The effects of this difference have to be taken into consideration and analyzed in order to correlate the bulk and bonded fracture toughness and energy values of Metlbond 1113 adhesive. Another interesting area of future research will be the analytical correlation of cure conditions with the resulting microscopic changes in the adhesive molecular structure and the observed macroscopic effects such as strength, fracture toughness, energy etc.

Acknowledgements

The material covered in this paper is based upon work supported by the National Science Foundation under Grant No. GME-8007251.

References

1. E. Sancaktar, H. Jozavi and R. M. Klein, *J. Adhesion* **15**, 241–264 (1983).
2. R. M. Klein, H. Jozavi and E. Sancaktar, Clarkson College of Technology, Report No. MIE-081, Potsdam, New York (1982).
3. E. Sancaktar and H. F. Brinson, Virginia Polytechnic Institute Report No. VPI-E-79-33 (1979).
4. D. W. Dwight, E. Sancaktar and H. F. Brinson, *Polymer Science and Technology Series, Vol.* 12-*A, Adhesion and Adsorption of Polymers*, L. H. Lee, Ed. Plenum Press, NY (1980), pp. 141- 164.
5. R. C. Bowers and W. A. Zisman, *Engineering Design for Plastics*, E. Baer, Ed. (Reinhold Book Corp., New York, 1964), pp. 689–741.
6. W. D. Bascom, C. O. Timmons and R. L. Jones, *J. Materials Science*, **10**, 1037–1048 (1975).
7. S. Mall, W. S. Johnson and R. A. Everett Jr., NASA Technical Memorandum (1982).
8. D. G. O'Connor, "Factors Affecting the Fracture Energy for a Structural Adhesive," Master's Thesis, Virginia Polytechnic Institute and State University, Blacksburg, VA (1979).
9. E. Sancaktar and H. F. Brinson, *Polymer Science and Technology Series, Vol.* 12-*A, Adhesion and Adsorption of Polymers*, L. H. Lee, Ed. (Plenum Press, NY, 1980), pp. 279–300.
10. H. F. Brinson, M. P. Renieri and C. T. Herakovich, *Fracture Mechanics of Composites*, ASTM STP 593, (ASTM, Philadelphia, 1975), pp. 177–199.
11. M. P. Renieri, C. T. Herakovich and H. F. Brinson, Virginia Polytechnic Institute Report No. VIP-E-76-7 (1976).
12. L. J. Hart-Smith, Air Force Conference on Fibrous Composites in Flight Vehicle Design, Dayton, Ohio (1972).
13. W. D. Bascom, R. L. Cottington and C. O. Timmons, *Naval Engineering Journal* **88**, 73–86 (1976).
14. W. D. Bascom, R. L. Cottington and C. O. Timmons, *J. Applied Poly. Sci.: Applied Polymer Symposia* **32**, 165–188 (1977).
15. W. D. Bascom and R. L. Cottington, *J. Adhesion* **7**, 333–345 (1976).
16. W. D. Bascom, *et al.*, *J. Appl. Polym. Sci.* **19**, 2545–2562 (1975).
17. W. D. Bascom, R. L. Jones and C. O. Timmons, *Adhesion Science and Technology*, Vol. 9B, pp. 501–511 (1975).
18. R. O. Ebewele, B. H. River, J. A. Koutsky, *J. Adhesion* **14**, 189–217 (1982).

19. A. J. Kinloch, *Developments in Adhesives*-2 (Applied Science Publishers, London, 1981), pp. 83–124.
20. G. R. Irwin, *Applied Materials Research* **3**, 65 (1964).
21. G. R. Irwin and P. C. Paris, *Fracture-An Advanced Treatise, Vol.* 3, H. Liebowitz, Ed. (Academic Press, New York, 1971), p. 676.
22. G. R. Irwin, *Proc. 7th Sagamore Conf.*, p. 4–63 (1960).
23. S. Mostovoy, E. J. Ripling and C. F. Bersch, *J. Adhesion* **3**, 125 (1971).
24. S. Mostovoy, P. B. Crosley and E. J. Ripling, *J. Materials* **2**, No. 3, 661–681 (1967).
25. W. F. Brown Jr., J. E. Strawley, *ASTM STP* 410 ASTM, Philadelphia, (1966).
26. *ASTM E:* 399-81, "Standard Test Method for Plane-Strain Fracture Toughness of Metallic Materials."
27. Metlbond 1113 Adhesive product Information Brochure, Narmco Materials Division, Whittaker Corp., Costa Mesa, California.
28. B. Gross, J. E. Strawley, W. F. Brown Jr., Technical Note D-2395, NASA (1964).
29. M. L. Williams, Trans. ASME *J. Appl. Mechanics* **24**, 109–114 (1957).

NOMENCLATURE

K_{Ic}	plain strain critical stress intensity factor in Mode-I failure (fracture toughness)
G_{Ic}	plain-strain critical strain energy release rate in Mode-I failure (fracture energy, crack extension force)
E	elastic modulus
ν	Poisson's ratio
r_p	diameter of crack tip plastic zone
r_{yc}	plane-strain crack tip plastic zone radius
σ_y	yield strength
a	crack length
B	specimen thickness
Y	the K-calibration factor
w	specimen width
P_c	critical load at fracture initiation
$\bar{r}_{yc}$	average plastic zone radius